agronomy

MDPI

Article

Fabrication and Characterization of ZnO Nanoparticles-Based Biocomposite Films Prepared Using Carboxymethyl Cellulose, Taro Mucilage, and Black Cumin Seed Oil for Evaluation of Antioxidant and Antimicrobial Activities

Abonti Biswas [1], Tanvir Ahmed [1], Md Rahmatuzzaman Rana [1,*], Md Mozammel Hoque [1], Md Farid Ahmed [2], Minaxi Sharma [3], Kandi Sridhar [4], Rowshon Ara [1] and Baskaran Stephen Inbaraj [5,*]

1 Department of Food Engineering and Tea Technology, Shahjalal University of Science and Technology, Sylhet 3100, Bangladesh
2 Institute of Glass and Ceramic Research and Testing (IGCRT), Bangladesh Council of Scientific and Industrial Research (BCSIR), Dhaka 1205, Bangladesh
3 Haute Ecole Provinciale de Hainaut-Condorcet, 7800 Ath, Belgium
4 Department of Food Technology, Koneru Lakshmaiah Education Foundation Deemed to be University, Vaddeswaram 522 502, Andhra Pradesh, India
5 Department of Food Science, Fu Jen Catholic University, New Taipei City 242062, Taiwan
* Correspondence: rzaman-fet@sust.edu (M.R.R.); sinbaraj@yahoo.com or 138547@mail.fju.edu.tw (B.S.I.)

Abstract: Food packaging is often made from plastic, which is usually obtained from non-renewable resources. The development of new technologies, like biocomposite films, has been driven in response to environmental concerns as well as consumer demands for eco-friendly, high-quality products derived from nature. Biocomposite films were prepared by incorporating taro mucilage, carboxymethyl cellulose (CMC), ZnO, glycerol, and black cumin seed (BCS) oil. The SEM results showed that the biocomposite films containing taro mucilage (TM), ZnO, and BCS oil had noticeably smoother surfaces. The FTIR analysis indicated the existence of a -OH group, N-H bond, alkaline group, C-C, C=N, C-H, C-O-H, and C-O-C bond formation, confirming the interaction of CMC, glycerol, BCS oil, ZnO nanoparticles, and TM. The results of TGA and DSC analysis suggest that incorporating ZnO nanoparticles, BCS oil, and TM into the CMC polymer matrix increased thermal stability. The addition of TM significantly increased water uptake capacity, antioxidative property, tensile strength, and elongation at break, with significantly decreased whiteness index and water solubility. The film inhibited the growth of *Staphylococcus aureus* and *Escherichia coli* as foodborne pathogens. The results suggest that the films can be potentially used as environment-friendly antioxidative and antimicrobial packaging films with additional research.

Keywords: biocomposite films; taro (*Colocasia esculenta*) mucilage; ZnO; CMC; black cumin; film properties

Citation: Biswas, A.; Ahmed, T.; Rana, M.R.; Hoque, M.M.; Ahmed, M.F.; Sharma, M.; Sridhar, K.; Ara, R.; Stephen Inbaraj, B. Fabrication and Characterization of ZnO Nanoparticles-Based Biocomposite Films Prepared Using Carboxymethyl Cellulose, Taro Mucilage, and Black Cumin Seed Oil for Evaluation of Antioxidant and Antimicrobial Activities. *Agronomy* **2023**, *13*, 147. https://doi.org/10.3390/agronomy13010147

Academic Editor: Jesús Martín-Gil

Received: 19 December 2022
Revised: 28 December 2022
Accepted: 29 December 2022
Published: 2 January 2023

1. Introduction

The total volume of food packaging materials used today exceeds 200 million tons per year, with an annual increase of about 5% [1]. Currently, enormous quantities of food packaging are dumped into the environment, making the waste problem worse each year. Therefore, alternative materials must replace conventional, non-recyclable, or non-biodegradable packaging to solve numerous ecological issues. In this aspect, biodegradable and eco-friendly biopolymer-based packaging is the ideal contender for lowering the enormous volume of conventional plastics. Recently, the biodegradable film generated from hydrocolloid compounds has received the most attention due to its biodegradability and edible properties. However, the biodegradable films' use is limited by their brittleness and weak resistance to gas exchange [2]. This factor, along with environmental concerns and consumer demands for high quality eco-friendly products related to those found in

nature (natural products), has driven the development of new technologies, such as the production of biocomposite films. Using plant-derived materials with antioxidant and antimicrobial properties in biocomposite films as a sustainable strategy for maintaining and/or extending the shelf life of food products has been promising [3].

Natural biopolymers, such as cellulose, are currently attracting particular attention in the food packaging industry due to the increased demand for environmentally friendly products from customers and manufacturers. Cellulose is one of the most promising materials for developing biocomposite films. Cellulose is the most abundant, renewable, and biodegradable substance and has a linear polysaccharide consisting of repeated units of β-(1–4) linked D-glucose [4]. For food packaging, processing, and pharmaceutical industries, carboxymethyl cellulose (CMC) is the most common cellulose derivative because of its outstanding film formability, stable internal network structure, and strong gas barrier properties, biocompatibility, and hydrophilicity. Additionally, CMC has been utilized to enhance the qualities of polymer-based composite films and edible coatings that extend the shelf life of food [5].

It is worth mentioning that poor moisture resistance and limited mechanical properties are the most frequent challenges in developing biocomposite films [6]. To address this issue, mucilage can be utilized as an alternative to a binary polymer to enhance the mechanical properties of a biocomposite film. Moreover, mucilage has been exploited as a stabilizer and thickening agent in the food and pharmaceutical industries due to its excellent viscosity, water-holding capacity, and antimicrobial activity. Among the plant kingdom, taro (*Colocasia esculenta*) is a potential source of about 4 to 20% mucilage and 80 to 90% starch. In addition, taro mucilage (TM) has better emulsifying properties because partially or completely hydrophobic amino acids in TM contain radicals. It is believed that the hydrophobic portion of TM is attributable to fractions of proteins containing non-polar radicals, whereas the hydrophilic portion is due to carbohydrates [7].

On the other hand, a plasticizer makes brittle films more flexible, but they are less intense and are more prone to moisture absorption. In this case, glycerol can dramatically affect the films' tensile and barrier properties. In addition, the lower glycerol content of the films, the tensile strength, and barrier properties will be better than films with higher content [8].

Nonetheless, extending a food's shelf life by inhibiting microbial growth and preventing undesirable biological or chemical changes remains one of the biggest hurdles in food packaging. Thus, the use of antimicrobial agents and antioxidants in packaging films is of particular interest for food packaging applications. In the production of antibacterial packaging films, various metal and metal oxide nanoparticles have already been utilized as antibacterial agents, including ZnO, Cu, Ag, TiO_2, and CuO. Moreover, the production of antioxidant packaging materials has used various antioxidants such as the natural pigments of anthocyanin, curcumin, and melanin, and essential oils and plant extracts [9]. Therefore, antimicrobial agents and antioxidants can be used together to produce biocomposite films with antimicrobial and antioxidant properties. For this purpose, ZnO nanoparticles can be used as antimicrobial agents to develop biocomposite films because of their higher thermal stability and less cytotoxicity.

Furthermore, it has been shown that ZnO nanoparticle antibacterial activity is primarily related to the destruction of cell membrane structures, diffusion of ions from the surface of nanoparticles, and binding to the cell membrane [10]. On the other hand, black cumin (*Nigella sativa* L.) seed oil (BCS oil) can be utilized as a potential antioxidant agent due to the predominant antioxidative compounds such as thymoquinone (30% of total volatile oil). Additionally, BCS oil also possesses numerous advantages, including hydrophilic properties, easy extraction, low cost, relative abundance, and biocompatibility compared to artificial ones [11]. Therefore, adding ZnO and BCS oil to biocomposite films is anticipated to improve the films' characteristics and impart antibacterial and antioxidant properties.

It is hypothesized that using biocomposite films for food packaging not only protects food and extends its shelf life but also reduces environmental pollution by eliminating the usage of plastic packaging materials. Realizing the importance of biocomposite film, an attempt has been made in this study to prepare CMC/TM/BCS oil-based biocomposite films

containing ZnO nanoparticles as well as glycerol and to investigate the physico-mechanical properties, antioxidant activity, and antibacterial activity of the prepared biocomposite films.

2. Materials and Methods

2.1. Materials

Fresh taro (*Colocasia essculenta*) corms were collected from Bangladesh Agricultural Development Corporation (BADC) Agro Service Center, Kumargaon, Sylhet, Bangladesh. Synthesized ZnO nanoparticles were provided by the Department of Chemistry, Shahjalal University of Science and Technology (SUST), Bangladesh. BCS oil was brought from a renowned super shop. *Escherichia coli* and *Staphylococcus aureus* were provided by the Department of Biochemistry and Molecular Biology, SUST. All the chemical compounds utilized were of analytical reagent grade and collected from Sigma-Aldrich (Burlington, MA, USA) and Merck (Darmstadt, Germany).

2.2. Taro Sample Collection and Preparation

After collecting and sorting, fresh taro corms were rinsed with distilled water to remove dirt and sand. Then the taro corms were peeled out using a stainless-steel knife. After that, the peeled taro corms were sliced into small surface area pieces.

2.3. Extraction of Taro Mucilage (TM)

The microwave extraction method was followed by some modifications for TM extraction [12]. Sliced taro corms were weighted to 100 gm. After weighing, they were soaked in a beaker with 550 mL distilled water for 2 h. Then the beaker was kept in the microwave (Model: Farberware Countertop Microwave Oven, Farberware, Fairfield, CA, USA) at 450 °C for 7 min. The supernatant was collected after centrifugation at 4000 rpm for 10 min. The aqueous TM solution was precipitated in a 1:3 volume of acetone (aqueous solution: acetone). The precipitate substances were filtered with filter paper no. 1. Then the aqueous and semi-liquid mucilage substances were placed carefully in a Petri dish and dried in a constant temperature and humid chamber (Model: VS-8111H-150, input 220 V 50 Hz 16 A 1 phase, Vision Scientific Co. Ltd., Yuseong-Gu, Daejeon-Si, South Korea) at 60 °C for 18 h. Dried TM was collected carefully and then kept in a desiccator.

2.4. Preparation of Biocomposite Films Based on CMC/ZnO/TM/BCS Oil

According to Table 1, biocomposite films were made using the solvent casting method [13]. According to our knowledge, a specific study on biocomposite film composed of CMC, TM, BCS oil, and ZnO nanoparticles has not yet been presented. As a foundation for future research, the present work aims to evaluate the influence of varied CMC and TM concentrations on the biocomposite film properties. Therefore, the concentrations of TM, CMC, ZnO, glycerol, and BCS oil were arbitrarily chosen. To prepare CMC film, first we dissolved the 2 g of CMC in 100 mL of distilled water and then mixed continuously for 5 min at 100 rpm with a homogenizer (Model: HG-15D-Set A-230V, Daihan, Korea). Afterward, 1 g/100 mL of glycerol was dissolved into the solution. Later, the homogenized solution was centrifuged at 4000 rpm for 10 min to remove air bubbles.

Table 1. Composition of the biocomposite film-forming solutions [1].

Batch Code	CMC (g/100 mL)	TM (g/100 mL)	ZnO (g/100 mL)	Glycerol (g/100 mL)	BCS Oil (g/100 mL)
F1	2.0	-	-	1.0	-
F2	2.0	-	0.5	1.0	-
F3	2.0	-	0.5	1.0	1.0
F4	1.4	0.6	0.5	1.0	1.0
F5	1.2	0.8	0.5	1.0	1.0
F6	1.0	1.0	0.5	1.0	1.0

[1] CMC, carboxymethyl cellulose; TM, taro mucilage; ZnO, zinc oxide; BCS: black cumin seed.

ZnO nanoparticles (0.5 g/100 mL per film-forming solution) were dispersed into distilled water to prepare a composite with ZnO and CMC (CMC/ZnO). After that, a mixture solution was formed by adding 2 g CMC and homogenized. The solution was centrifuged at 4000 rpm for 10 min to remove air bubbles. The same procedure was followed while adding 1 g/100 mL of black cumin seed oil to prepare CMC/ZnO/BCS oil composite film.

To prepare CMC/ZnO/BCS oil/TM, at first, precise weighted CMC (1, 1.2, 1.4, 2 g/100 mL), ZnO (0.5 g/100 mL), and TM (0.6, 0.8, 1 g/100 mL) were dispersed in 100 mL of deionized water. After pre-heating in an ultrasonic water bath at 60 °C for 20 min, then with an ultrasonic homogenizer (Ultrasonic Processor FS-200T, Hanchen, China), the solutions were mixed vigorously for 15 min at 80 W. To integrate more precisely, they were homogenized at 100 rpm. Finally, 1 g/100 mL of black cumin seed oil and 1 g/100 mL of glycerol were injected with a micropipette. A centrifuge (4000 rpm for 10 min) was then used to remove air bubbles from the film solutions.

All film solutions were equally cast onto a flat Petri dish and then dried for about 16 h at 60 °C in a Constant Temp and Humid Chamber (Model: VS-8111H-150, input 220 V 50 Hz 16 A 1 phase, Vision Scientific Co., Ltd., South Korea). To pour the same quantity of each treatment onto each panel, a consistent amount (film weight to plate area 1:3) of the film-forming solution was used. Then, the formed films were peeled away from the casting surface. The prepared films were kept in zip bags until further tests. Every film was coded as F1, F2, F3, F4, F5, and F6 per their CMC/ZnO/TM/BCS oil composition.

2.5. Characterization of Biocomposite Films

2.5.1. Appearance and Surface Color Measurements

The film's color was measured using a colorimeter (Model: PCE-CSM4, PCE Instruments, Southampton, UK) following the technique by Marvdashi et al. [14] with some modifications. Film specimens were put on the white standard plate (L* = 88.23, a* = 8.03, and b* = −5.56), and the degree of lightness (L*), redness (a*) or greenness (a*), and yellowness (b*) or blueness (b*) of the films were measured. The following Equation (1) was used to calculate the overall color difference (ΔE). Three readings were taken on either side of each film piece.

$$\Delta E = [(L_{film} - L_{standard})^2 + (a_{film} - a_{standard})^2 + (b_{film} - b_{standard})^2]^{1/2} \quad (1)$$

2.5.2. Whiteness Index Measurement

Packaging materials, plastics, and photographic paper each have whiteness indexes. Thus, the whiteness index connects visual assessments of whiteness for particular white and near-white surfaces, such as glass. The ASTM defines whiteness and yellowness indexes. The E313 whiteness index measures opaque near-white materials, including paper, paint, and plastic. In reality, this index applies to any substance that seems white. For example, if a flawless reflecting surface does not absorb or transmit light but instead reflects it at equal powers in all directions, it is described as white. The color of this kind of surface is known as preferred white for the reasons behind this norm. The whitening index was calculated from L (lightness), a (greenness), and b (yellowness or blueness) values according to Equation (2). The following equation was also used to obtain the whitening index of the biocomposite films. Three readings were taken on either side of each film piece [15].

$$\text{Whiteness index} = \left[100 - \sqrt{\left[(100 - L)^2 + a^2 + b^2\right]}\right] \quad (2)$$

2.5.3. Thickness and Mass

The thickness of biocomposite films was measured using a thickness gauge (Model: 2364-10, INSIZE, Suzhou New District, China) with a precision of 0.01 mm [16]. Each film was placed in the lower part, and the gap was filled with the grip. The Equation (3) was

used to calculate the thickness. The mass of the films was precisely weighed in triplicate using an electronic balance.

$$\text{Thickness (mm)} = (\text{Reading with sample} - \text{Reading without sample}) \times 0.01 \text{ mm} \quad (3)$$

2.5.4. Moisture Content

Moisture content has been determined according to the method described by Rhim and Wang [17] through the drying oven technique with some modifications. First, the rectangular films were cut into 3 cm × 3 cm squares and dried in a forced convection oven (Model: OF-21E, Jeio Tech, Korea) for 24 h at 105 °C. Then, the moisture content was determined using the weight loss after drying according to the Equation (4) and represented as a percentage.

$$\text{Moisture content (\%)} = \left[\left(\frac{\text{Initial sample weight (g)} - \text{weight of sample after drying (g)}}{\text{Initial sample weight (g)}}\right) \times 100\right] \quad (4)$$

2.5.5. Water Activity

The unbound water vapor pressure of the films was determined with a handheld water activity meter (Model: WA-60A, Amtast, Lakeland, FL, USA). The individual film samples were placed in the sample plates with affixing. The non-conductive humidity sensor was placed on the sample. When the vapor pressure of the water in the films and the water in the air approach equilibrium, the relative humidity of the air around the sample equals the water activity of the piece and is automatically shown on the monitor.

2.5.6. Water Solubility

The water solubility of biocomposite films was determined according to a method developed by Fernandes et al. [18] with some modifications. The materials were cut into 1 cm × 1 cm pieces and left to dry at 105 °C. Dried film specimens were soaked in distilled water (30 mL) and shaken for 1 h at 200 rpm in a shaking incubator (Model: SI-150, Hanyang Science Lab Co., Ltd., Seoul, Korea). The insoluble debris was separated and dried for 24 h at 105 °C. The following Equation (5) was used to calculate each biocomposite film's water solubility percentage.

$$\text{Water solubility (\%)} = \left[\left(\frac{\text{Initial dry weight of the film (g)} - \text{final dry weight of the film (g)}}{\text{initial dry weight of the film (g)}}\right) \times 100\right] \quad (5)$$

2.5.7. Water Uptake Capacity

The water uptake capacity of the biocomposite films was evaluated by following the methods described by Ghazihoseini et al. [19] and Foghara et al. [10] with slight modifications. The films were trimmed to 20 mm × 20 mm and put in a desiccator with calcium chloride powder (to eliminate moisture) for 24 h. The sliced films were weighed and put in a desiccator with water for 24 h. The films were weighed, and the quantity of water absorption was calculated according to the Equation (6):

$$\text{Water uptake capacity (\%)} = \left[\left(\frac{P - Q}{Q}\right) \times 100\right] \quad (6)$$

where P = weight of films after being in contact with H_2O of the desiccator (g) and Q = weight of films after being in contact with $CaCl_2$ of the desiccator (g).

2.5.8. Mechanical Properties

A tensile strength test was carried out to evaluate the mechanical properties of the biocomposite films following the guidelines provided by the American Society for Testing and Materials (ASTM Standard, 2003) with a few adjustments [20]. Each film was divided into three replicate samples that were 8 cm × 1.5 cm in size. Before conducting tensile strength studies, the texture analyzer (Model: Z10-700, AML Instruments, Lincolnshire,

UK) was calibrated using a 5 kg load. A 2 cm line was drawn at both ends of the film strips. The starting separation distance was set at 40 mm and the velocity was maintained at 0.40 mm/second. The trigger force was automatically set to 300 mm/minute before testing and 600 mm/minute following testing. The texture analyzer had a cell load capacity of 30 kg and its return distance was 190 mm. The tensile strength (TS), as well as the elongation at break (EB), were obtained by directly analyzing the stress-strain curves with the Texture Exponent 32 software V.4.0.5.0. (SMS) and calculated according to the Equations (7) and (8).

$$\text{TS (MPa)} = \left[\frac{\text{Maximum force at break (N)}}{\text{Biocomposile film surface (mm}^2\text{)}}\right] \quad (7)$$

$$\text{EB (\%)} = \left[\left(\frac{\text{Length extended at breaking point of sample (mm)} - \text{Initial length of sample (mm)}}{\text{Initial length of sample (mm)}}\right) \times 100\right] \quad (8)$$

2.5.9. Analysis of Fourier Transform-Infrared (FT-IR) Spectroscopy

Film samples were analyzed using an ATR-FTIR spectrophotometer (Model: MIRacle 10, IR Prestige21, Shimadzu Corporation, Japan) with a wavenumber of 4000–400 cm^{-1} and a resolution of 30 scans at 4 cm^{-1}. Film samples (5 × 5 cm) were put instantly on the beam exposure stage and evaluated for measurement [21].

2.5.10. Scanning Electron Microscopy (SEM)

The surface morphology of specified films was analyzed using a scanning electron microscope (Model: Phenom Pro Desktop SEM/Prox G6, nanoscience Instruments, Arizona, USA) with a magnification of 50 µm. The stub pin was inserted with a sample of 180 µm into the hole on the monitoring surface. The height adjustment for the sample holder was monitored and then positioned correctly. After activating the optical camera, the image was displayed in the main viewing window of the image screen; 5 kV was set for the operation and the image was autofocused. Finally, the microstructure for each film was collected.

2.5.11. Thermal Properties

A synchronous thermal analyzer (Model: STA449F3, NETZSCH, Weimar, Germany) was used to determine the thermal properties of films (TGA and DSC). Films were heated at a constant rate of 10 °C/min from 30 °C to 600 °C under nitrogen.

2.6. Antioxidant Activity of Biocomposite Films (DPPH Method)

The antioxidant potential of CMC-based biocomposite film samples was evaluated utilizing DPPH extremists [22]. It was necessary to create the extract by dissolving 0.1 g of the film specimens in 10 mL of distilled water. After being vortexed for 3 min, the solution was put in a shaking incubator for 30 min to finish the process. After 30 min, the samples were centrifuged at 2700× *g* for 10 min to separate the components. After that, the supernatant was decanted to measure DPPH radical scavenging activity. Next, 0.1 mL film extraction solution was added to a 0.1 mM 3.9 mL DPPH solution, which resulted in a final concentration of 0.1 mM. The solution is vortexed once more before being stored in a dark chamber. The solution's absorbance was measured using a UV-Vis spectrophotometer (Model-T60U, PG instruments limited, Leicestershire, UK) at a wavelength of 517 nm [23].

2.7. Antimicrobial Activity of the Biocomposite Films

Determining the inhibition zone of biocomposite against bacteria is an essential parameter in any active packaging. The antibacterial activity of film samples was determined by plating them on an agar medium [24]. The films were tested for their ability to suppress the growth of *Staphylococcus aureus* (a Gram-positive organism) and *Escherichia coli* (a Gram-negative organism). The susceptibility of control *E. coli* and *S. aureus* isolates to a panel of samples (F1, F2, F3, F4, F5, and F6) and was determined by using the Kirby–Bauer disc diffusion method on Mueller–Hinton Agar plates according to the guidelines and

breakpoints of the Clinical and Laboratory Standard Institute [25]. The plates were loaded well with nighttime bacterial isolate at a level of 1.0×10^6 (100 µL) CFU/mL. The films were trimmed to 6 mm diameter discs using a hole puncher. Then, the film was inserted in the exact center bearing already infested agar. After incubating at 37 °C for 24 h, the clear zone generated in the media around the film sample was measured with a caliper. The inhibition area diameter was obtained by eliminating each film region from the entire zone. Every evaluation of the inhibition test was conducted in triplicate. The mean ± standard deviation of triplicates was utilized as the outcome of each test.

2.8. Statistical Analysis

The film properties were measured in triplicate with individually prepared films as replicated experimental units. One-way analysis of variance (ANOVA) was performed, and the significance of each mean property value was determined ($p < 0.05$) by the Tukey honestly significant difference (HSD) test using the SPSS statistical analysis program for Windows (SPSS Inc., Chicago, IL, USA).

3. Results and Discussion

3.1. Appearance and Surface Color of Biocomposite Film

Figure 1 and Table 2 illustrate the visual and color characteristics of the prepared biocomposite films. Biocomposite films' color properties were affected by the addition of TM, BCS oil, and ZnO nanoparticles. Figure 1 shows that the surface of the biocomposite film F1 was generally colorless and transparent. The film became whiter after the addition of ZnO nanoparticles. It indicated the formation of ZnO nanoparticles. A similar type of surface appearance was also observed when ZnO nanoparticles were added into rice-starch/ZnO nanoparticles-based antimicrobial film [26]. Additionally, BCS oil added to F3 caused the surface to roughen more than F2, and the biocomposite films (F4, F5, F6) that contained TM together with ZnO nanoparticles and BCS oil had noticeably smoother surfaces, demonstrating that the TM concentration in the solution used to make the film served as a leveling agent.

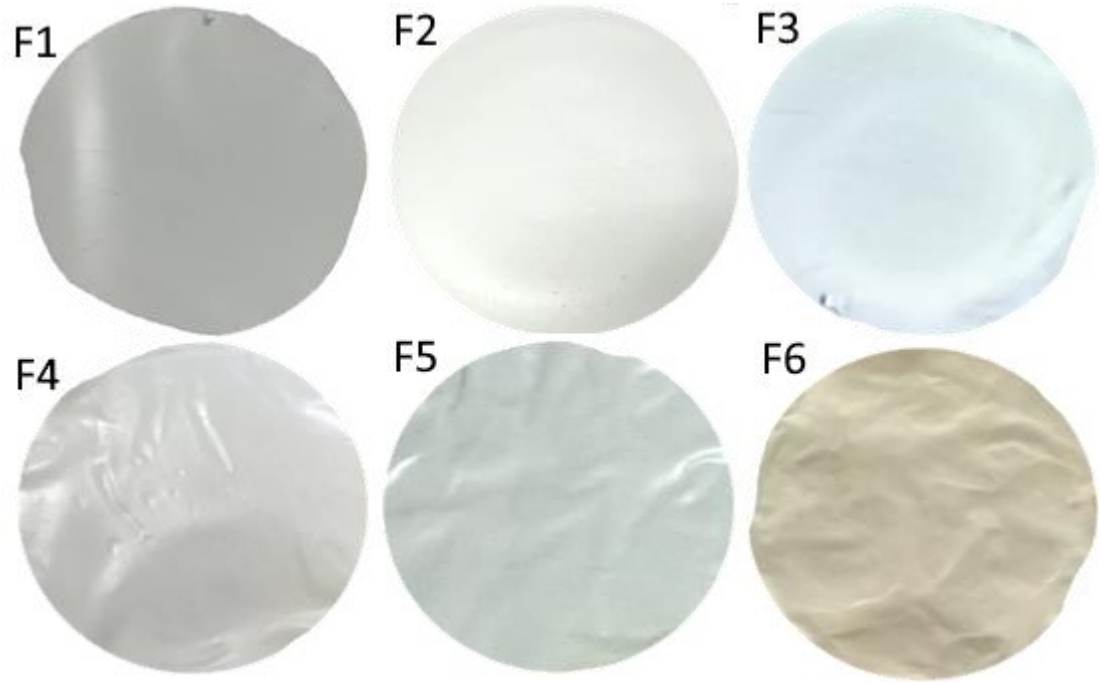

Figure 1. The visual appearance of the biocomposite films incorporated with CMC and TM concentrations with ZnO nanoparticles, BCS oil, and glycerol. CMC, carboxymethyl cellulose; TM, taro mucilage; ZnO, Zinc oxide; BCS: black cumin seed. For sample codes F1 to F6, refer to Table 1.

Table 2. Physico-mechanical and antioxidative properties of the biocomposite films [1].

Parameters	F1	F2	F3	F4	F5	F6
Mass (g)	0.75 ± 0.13 [a]	0.96 ± 0.13 [ab]	1.37 ± 0.19 [c]	1 ± 0.08 [b]	0.86 ± 0.02 [ab]	0.96 ± 0.03 [ab]
Thickness (mm)	0.13 ± 0.02 [a]	0.15 ± 0.04 [a]	0.20 ± 0.03 [a]	0.20 ± 0.09 [a]	0.17 ± 0.05 [a]	0.15 ± 0.03 [a]
Moisture content (%)	25.38 ± 0.10 [a]	22.07 ± 0.19 [b]	20.43 ± 0.34 [c]	29.30 ± 0.22 [d]	33.21 ± 0.44 [e]	38.32 ± 0.12 [f]
Water activity (%)	0.21 ± 0.01 [a]	0.06 ± 0.01 [b]	0.09 ± 0.02 [c]	0.10 ± 0.01 [c]	0.20 ± 0.02 [a]	0.21 ± 0.02 [a]
Water solubility (%)	88.96 ± 4.00 [a]	75.33 ± 2.52 [b]	57.45 ± 0.51 [c]	45.89 ± 2.77 [d]	34 ± 2.65 [e]	37.33 ± 3.21 [e]
Water uptake capacity (%)	274.67 ± 43.59 [a]	215.70 ± 49.75 [b]	152.81 ± 35.41 [c]	158.19 ± 5.97 [c]	365 ± 12.87 [d]	363.92 ± 5.55 [d]
Antioxidative activity (%)	20.76 ± 0.03 [a]	24.14 ± 0.01 [b]	31.11 ± 0.04 [c]	37.61 ± 0.02 [d]	44.04 ± 0.04 [e]	65.63 ± 0.01 [f]
Tensile strength (MPa)	7.54 ± 1.03 [ab]	11.80 ± 4.94 [c]	13.17 ± 0.48 [c]	14.41 ± 0.65 [c]	11.29 ± 1.92 [bc]	6.29 ± 0.64 [a]
Elongation at break (%)	12.39 ± 4.60 [a]	45.52 ± 11.59 [b]	31.54 ± 6.25 [c]	52.8 ± 1.92 [b]	65.64 ± 4.86 [d]	50.99 ± 6.04 [b]
Surface color						
L*	81.45 ± 0.43 [a]	88.33 ± 0.77 [b]	88.48 ± 0.36 [b]	77.21 ± 0.99 [c]	78.39 ± 1.18 [c]	88.28 ± 0.20 [b]
a*	7.90 ± 0.01 [a]	7.90 ± 0.01 [a]	8.19 ± 0.03 [a]	9.82 ± 0.01 [b]	10.77 ± 0.09 [c]	11.38 ± 0.35 [d]
b*	−4.00 ± 0.01 [a]	0.06 ± 0.01 [b]	7.27 ± 0.04 [c]	8.32 ± 0.09 [d]	10.47 ± 0.04 [e]	13.15 ± 0.21 [f]
Color difference (ΔE)	6.96 ± 0.42 [a]	8.28 ± 3.68 [a]	12.83 ± 0.04 [b]	17.28 ± 0.36 [c]	16.30 ± 0.02 [c]	22.55 ± 0.30 [d]
Whiteness index	79.44 ± 0.39 [a]	89.90 ± 0.63 [b]	85.91 ± 0.17 [c]	80.96 ± 0.10 [d]	74.60 ± 1.12 [e]	71.33 ± 0.85 [f]

[1] Data are mean ± standard deviation (SD). Mean values with different letters in a row indicate a significant difference at $p < 0.05$ using Tukey honestly significant difference test. L*, lightness; a*, red/green value; b*, blue/yellow value. For sample codes F1 to F6, refer to Table 1.

In Table 2, the measured color characteristics of the biocomposite films are presented. These parameters include ΔE (total color difference), L (lightness), a (green-red), and b (blue-yellow). Compared to the standard white plate, the CMC and glycerol-prepared film (F1) had the lowest ΔE value (6.96 ± 0.42). The addition of BCS oil, ZnO nanoparticles, and TM to the samples increased ΔE, resulting in more blurred films. The total color difference (ΔE) of the biocomposite films increased to 8.28 ± 3.68 (F2), 12.83 ± 0.04 (F3), 17.28 ± 0.36 (F4), 16.30 ± 0.02 (F5), and 22.55 ± 0.30 (F6). In a study on nanocomposite films prepared with CMC, okra mucilage, and ZnO nanoparticles, Mohammadi et al. [27] found that the film prepared with CMC had the lowest ΔE value (3.78 ± 0.37). The increasing mucilage content in the samples and the inclusion of ZnO nanoparticles contributed to a rise in ΔE.

The lightness (L value) of the F1 film was 81.45 ± 0.43; however, it considerably increased ($p < 0.05$) following integration with BCS oil and ZnO nanoparticles, reaching 88.33 ± 0.77 and 88.48 ± 0.36, respectively, in the F2 and F3 films. Even though the L value of the F4 and F5 biocomposite films dropped dramatically after TM was added, the color of the biocomposite films was remarkably improved when the concentration of TM was increased from 0.6 to 1.0 g/100 mL. Comparatively, the L values of the processed films ranged from 77.21 ± 0.99 to 88.48 ± 0.36. A higher L value indicates the reflection of light, which can protect foods susceptible to light or oxidation. In fact, light speeds up the oxidation and rancidification of pigments and vitamins, thereby reducing the nutritional value of foods [28].

As illustrated in Figure 1, the films had b color parameters that ranged from −4.00 ± 0.01 to 13.15 ± 0.21, which indicated that they had linen white to light yellow tint. Likewise, a slight increase in the value of a was also caused by ZnO nanoparticles and BCS oils, but an increase in TM concentration led to a significant increase in the value of a, which gave the films a faint reddish appearance. These findings may be attributable to polyphenols in BCS oil and TM, which imparted color and various light barrier properties to the biocomposite films [29].

3.1.1. Whiteness Index

The color analysis revealed that the effect of CMC, TM concentration, ZnO nanoparticles, and BCS oil had a significant impact on the whiteness index factor of the prepared biocomposite films. As shown in Table 2, adding ZnO nanoparticles to F2 film considerably increased the whiteness index (79.44 ± 0.39), likely due to the white color of the ZnO nanoparticles. In contrast, the whiteness index of the F2 film decreased significantly to 89.90 ± 0.63 after the addition of BCS oil. As essential oils in BCS oil are hydrophobic, they are slightly soluble in water, creating a heterogeneous film that causes turbidity. The reduction in the whiteness index of the film after the addition of essential oil was evident, and the

findings of this study are consistent with those of Ghamari et al. [15], Ojagh et al. [30], and Atares et al. [31]. Correspondingly, the increased TM concentration significantly decreased the films' whiteness index from 80.96 ± 0.10 (F4) to 71.33 ± 0.85 (F6). The increased starch concentration from TM addition made biocomposite films more opaque [32].

3.1.2. Surface Morphology of the Biocomposite Film Using SEM

The surface morphology characteristics of the biocomposite films were investigated using scanning electron microscopy (SEM), as shown in Figure 2. The surfaces of film F1, a mixture of CMC and glycerol, were smooth and homogeneous. The ability of glycerol to form hydrogen bonds makes it an ideal plasticizer for various applications. Thus, it is possible that CMC hydroxyl groups and glycerol formed hydrogen bonds within the film, reducing its surface free energy and increasing its contact angle [33]. Srikandace et al. [34] found that incorporation of CMC-glycerol in a bio-cellulose film produced smooth and homogeneous fibers with fewer pores. In contrast, the CMC/glycerol/ZnO nanoparticles film (F2) showed rough-surface structures. The SEM results revealed that the ZnO nanoparticles were equally dispersed throughout the films, with no particle agglomeration. Similar surface morphologies of nanocomposite films were found with ZnO nanoparticles' incorporation such as agar/ZnO nanoparticles, carrageenan/ZnO nanoparticles, CMC/ZnO nanoparticles [35], and gelatin/ZnO nanoparticles [36]. On the contrary, the film containing BCS oil (F3) exhibited a cracked structure and pores, possibly due to the evaporation of the essential oil from BCS oil during drying. This was also evident from a study by Muñoz-Tébar et al. [37], who reported that films comprised of chia mucilage and essential oil exhibited smooth surfaces devoid of pores or cracks, indicating that the film solution maintained a stable emulsion system after drying. The same results were also observed by Ghamari et al. [15], who found a pore and crack structure in the film's microstructure containing BCS oil. Interestingly, incorporating BCS oil reduced the surface roughness of the biocomposite films (F4, F5, and F6), and increasing the concentration of BCS oil made the surface smoother and had fewer pores. This property may be due to interactions between the starch of TM, glycerol, and CMC during the process of gelatinization with heating. In the film matrix, hydrocolloids assemble themselves, and hydrogen bonds may be disrupted during heating, resulting in the formation of the crystalline zone. During film preparation, the starch expanded, resulting in granule expansion and starch gelatinization. Similarly, Wang et al. [38] developed four films that contain CMC, glycerol, mucilage, and starch in different compositions. In the SEM analysis, dry films were characterized by their homogeneity and lack of defects or cracks, while having clear starch granules and a smooth structure [39]. It could be assumed that films with homogeneous matrix and fewer pores or cracks would have good mechanical properties, as well as better resistance to solvents and a lower permeance value to water vapor.

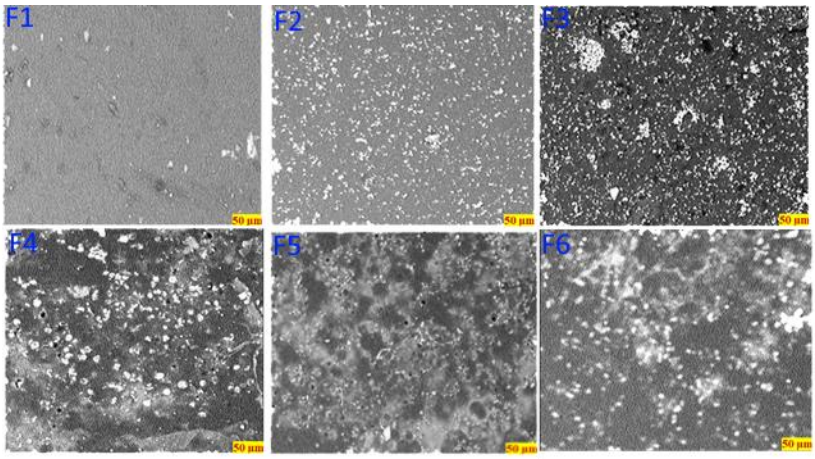

Figure 2. Micrographs of the biocomposite films with 50 μm magnification. For sample codes F1 to F6, refer to Table 1.

3.1.3. Chemical Structure Characteristics of the Biocomposite Film Using FT-IR

As shown in Figure 3, FT-IR spectra were used to identify the functional groups in biocomposite films. Comparing the spectra of all the films, no new peaks were found, meaning that no new chemical bonds were formed as a result of adding TM, BCS oil, or ZnO nanoparticles. Nonetheless, the different peak intensities suggest different contents of functional groups. All of the biocomposite films' spectra exhibited distinctive peaks within the region of 3340 to 570 cm^{-1}. Broad bands between 3500–3100 cm^{-1} in all samples pointed to the presence of hydroxyl groups (–OH) with intermolecular hydrogen stretching bonds. These types of interactions are typical of polysaccharides. Moreover, these bands may also suggest the presence of N–H bonds in proteins, as 30–51% of proteins were identified in the TM [40]. The peak around 2920 cm^{-1} was likely due to the stretching vibration of an alkane group within the biopolymer chain [21]. The β-casein-derived C–C or C=N appeared as a strong peak between 2200–2400 cm^{-1} [41]. The peak identified at 1592 cm^{-1} was attributed to the carboxyl group's asymmetric stretching vibration [21]. C–H bending vibrations and C–O–H of carboxylic acid may correspond to the band around 1414 and 1321 cm^{-1}, respectively [42,43]. It was determined that the C–O–H and C–O–C vibrations of the glycosidic bond in the TM were responsible for the peaks that were seen at 1110 cm^{-1} and 1045 cm^{-1}, respectively [44]. In the biocomposite film, it was found that peaks at 880 cm^{-1} and 831 cm^{-1} were caused by the C–H stretching of β-galactose residues. Alternatively, it may also result from C-H angular variation vibration of pyranoid sugar's α-epimerism [35,40]. Another vibrational band around 570 cm^{-1} may be associated with the skeletal mode vibration of the pyranose ring in the glucose unit [26].

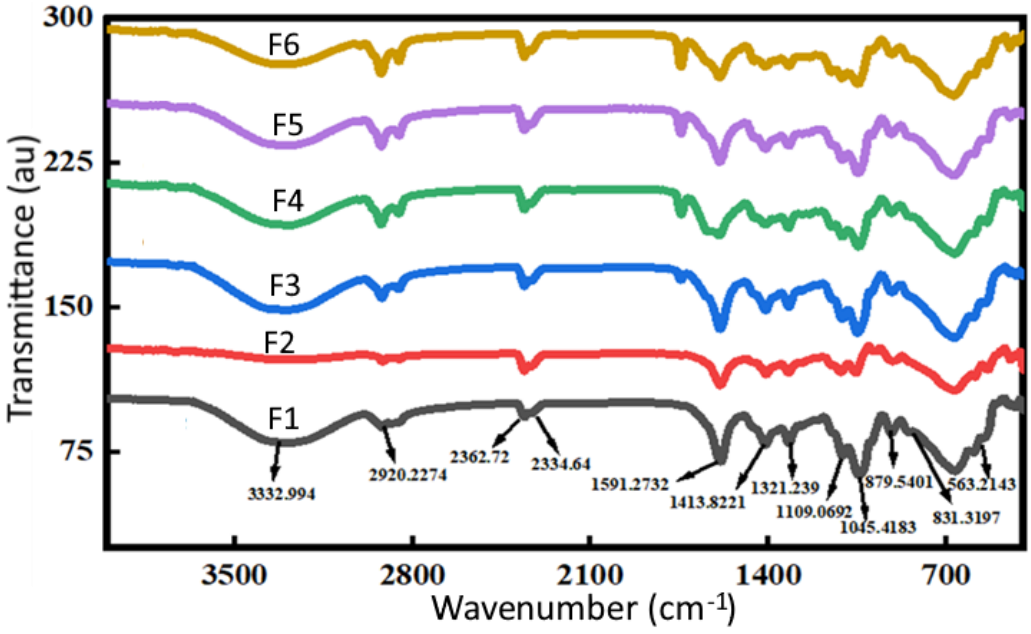

Figure 3. The FT-IR spectra of biocomposite films. For sample codes F1 to F6, refer to Table 1.

3.1.4. Thermal Properties

Figure 4a,b shows the thermogravimetric analysis at 30–600 °C, including thermogravimetry (TGA) and differential scanning calorimetry (DSC), respectively. A thermal analyzer determines the behavioral changes, fusion regions, and phase transition range. Figure 4a shows the TGA, which illustrates the weight loss stages. The TGA curve displayed three-step weight loss patterns. The first, weight loss, started at 50−100 °C due to desorption of moisture linked by hydrogen bonds to the polysaccharide structure [45]. The second stage of degradation occurred at 100−250 °C and corresponded to glycerol plasticizer, BCS oil, and CMC degradation from the complex [46]. The foremost degradation step at 260–350 °C was the decomposition of the polysaccharides of hemicellulose

in TM [47]. The fourth stage started near 350 °C, with a tendency to continue decreasing above 450 °C. The final stage suggested the decomposition of polymers in all samples [48]. It is clear from the findings that the inclusion of ZnO nanoparticles, BCS oil, and TM into the CMC polymer matrix displayed a stabilization influence against decomposition. This could be attributed to the adhesion between CMC polymer chains, ZnO nanoparticles, BCS oil, and TM, which enhanced thermal stability. Above 500 °C, the TGA curve stabilized, which corresponds to endothermic crystallization that allows the formation of mineral salts and ashes [49]. It is also worth noting that early weight gain in deterioration may be attributed to TGA equipment buoyancy. In TGA analysis, buoyancy is the upward push on the sample created by the surrounding atmosphere. With increasing temperature, the atmosphere's density drops, resulting in apparent mass gain.

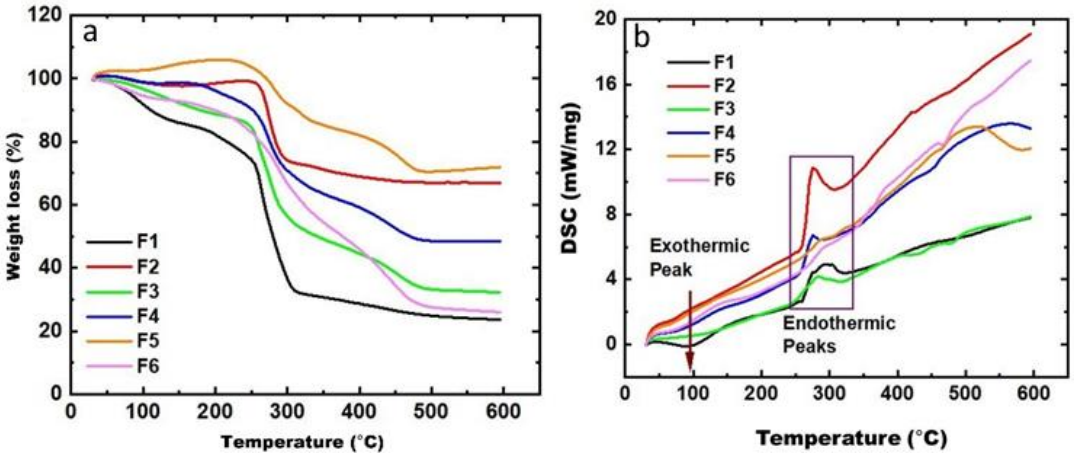

Figure 4. Thermogravimetric analysis of the biocomposite films: thermogravimetric analysis (**a**) and differential scanning calorimetry (**b**). For sample codes F1 to F6, refer to Table 1.

DSC thermograms of the prepared films are presented in Figure 4b. Three small endothermic and one exothermic transition were observed for each film. The first endothermic peak situated at approximately 50 °C may correspond to the water evaporation [38]. Similar values were found by Li et al. [40], where water evaporation started at approximately 80 °C from CMC/*Dioscorea opposite* mucilage/glycerol/ZnO nanoparticles-based edible films. The second endothermic peak in the range of 110–160 °C can be attributed to the evaporation of low molecular weight compounds such as glycerol or structurally bound water of the film network [50]. The third sharp endothermic peak in the range of 270–310 °C may correspond to the melting temperature of CMC [51]. On the other hand, the F1 (only CMC and glycerol) biocomposite films showed a sharp exothermic peak, whereas for the F2, F3, F4, F5, and F6 films, a slight decrease was noticed after the addition of ZnO nanoparticles, BCS oil, and TM. Moreover, a small exothermic peak appeared at a higher temperature (approximately 450–500 °C), which could be attributed to the release of inorganic materials like oxides, carbonaceous residues due to methylation [52]. Overall, the present observation suggests that incorporating ZnO nanoparticles, BCS oil, and TM into the CMC polymer matrix improved the thermal stability of prepared biocomposite films.

3.1.5. Thickness and Mass

Table 2 shows the thickness and mass of each film. Each film was analyzed in triplicate and the thickness was measured at five random locations. Film thickness varied from 0.13 ± 0.02 mm to 0.20 ± 0.03 mm. The addition of ZnO, BCS oil, and TM on a biocomposite film did not significantly affect film thickness. The results showed that adding ZnO nanoparticles and BCS oil increased the thickness of biocomposite films from 0.13 ± 0.02 mm (F1) to 0.20 ± 0.03 mm (F3). This phenomenon can be related to the increase in dry matter content of the matrix due to the addition of ZnO nanoparticles and BCS oil [53]. It can also be possible that the interactions between the CMC and the active compounds present in BCS

oil may have reduced the alignment of the polymer chains, reducing the compression of the network and consequently increasing the thickness of the films [54]. This result was consistent with Praseptiangga et al. [55] and Mohammadi et al. [27]. They reported an increase in the nanocomposite film thickness associated with an increase in the total solid content mass in the film matrix after adding ZnO nanoparticles. Lee et al. [56] also reported a significant increase in thickness in hydroxypropyl methylcellulose film containing oregano essential oil. In the present work, it has been observed that a correlation exists between the thickness and mass of the biocomposite films. The mass of films F, F2, F3 were 0.75 ± 0.13 g, 0.96 ± 0.13 g, and 1.37 ± 0.19 g, respectively, which indicated that adding ZnO nanoparticles and BCS oil increased the mass of the prepared biocomposite films significantly. Interestingly, increased concentration of TM and decreased concentration of CMC gradually declined the thickness (F4: 0.20 ± 0.09 mm-F6: 0.15 ± 0.03 mm) as well as mass (F4:1 ± 0.08 g-F6:0.96 ± 0.03 g) of the biocomposite films (not significantly). The hydrogen atom from the hydroxyl group (O–H) in the film matrix interacted with the oxygen atom from the nanoparticle molecules to form a hydrogen bond. Even though the concentration of CMC decreased, more hydrogen bonds were able to form when the concentration of TM increased. This led to a reduction in the availability of the hydroxyl groups in the polymer to interact with H_2O molecules, thereby reducing the amount of water bounded in the film matrix so that the thickness was also reduced [28].

3.1.6. Mechanical Properties

The mechanical properties of the prepared biocomposite films, including tensile strength and elongation at break, are presented in Table 2. The tensile strength of the F1 film (consisting of CMC and glycerol) was 7.54 ± 1.03 MPa. Biocomposite films containing ZnO nanoparticles and BCS oil have significantly improved tensile properties (F2: 11.80 ± 4.94 MPa; F3: 13.17 ± 0.48 MPa). As a result of uniform dispersion of ZnO nanoparticles in the CMC polymer matrix, CMC and ZnO form stronger bonds with each other through ion bonding, increasing the tensile strength [57] and the van der Waals force, which strengthens the intermolecular forces between ZnO nanoparticles and polysaccharide in BCS oil [58]. In agreement with our result, a chitosan/ZnO/Melissa officinalis essential oil nanocomposite film exhibited increased tensile strength after adding ZnO nanoparticles and Melissa officinalis essential oil to the chitosan polymer matrix [59]. Conversely, it was observed that with increasing TM concentration from 0.6 to 1.0 g/100 mL, the tensile strength decreased significantly (14.41 ± 0.65 MPa (F4), 11.29 ± 1.92 MPa (F5), and 6.29 ± 0.64 MPa (F6)). As a result of the intermolecular interaction between TM and CMC, the molecule structure of the TM-CMC mixture becomes less compact, resulting in a decrease in tensile strength. The addition of okra mucilage to CMC led to a decrease in the tensile strength of CMC/okra mucilage/ZnO nanoparticles-based nanocomposite films, which was in line with our findings [27].

Table 2 also shows a significant increase (from 12.39 ± 4.60% (F1) to 45.52 ± 11.59% (F2)) in the elongation at break of the film samples after the addition of ZnO nanoparticles, which can be attributed to the dispersion of ZnO nanoparticles, uniform distribution of ZnO nanoparticles, and decrystallization of ZnO nanoparticles in the polymer matrix [60]. A similar result was observed when adding ZnO nanoparticles into a CMC matrix [35]. The addition of BCS oil also significantly decreased the elongation at the break of the prepared biocomposite films (31.54 ± 6.25% (F3)). BCS oil created a compact structure by improving continuity in a network of polysaccharides, which caused the elongation at break to decrease. A study carried out by Sharma et al. [61] also found a decrease in elongation at break with the incorporation of the essential oregano oil in the PLA/PBAT (Poly (lactide)/poly (butylene adipate-co-terephthalate) blend film [61]. On the other hand, the elongation at break values of films first increased (F4: 52.8 ± 1.92%, F5: 65.64 ± 4.86%) and then decreased (F6: 50.99 ± 6.04%) as the addition ratio of TM increased. Perhaps this is due to interactions between protein chains and polysaccharide chains strengthening effects on the film matrix. Nevertheless, a high amount of TM caused a weakening of

interactions between polysaccharide chains and protein chains, lowering the extensibility of films and increasing rigidity. The same trending results were found after adding chia mucilage to blended films containing chia mucilage and gelatin [62].

3.1.7. Moisture Content and Water Activity

Results shown in Table 2 show that moisture content ranged from 20.43 ± 0.34% to 38.32 ± 0.12%. The statistical analysis revealed that CMC, ZnO nanoparticles, BCS oil, and TM substantially affect the moisture content of biocomposite films. A significant decrease in moisture content was observed after adding ZnO nanoparticles. Biocomposite films have lower moisture contents due to the relatively strong interaction between the glycerol, ZnO nanoparticles, and CMC, which leads to an increase in -OH bonds. In addition, it may also be associated with cation-dipole solid interactions between the ZnO atom and –OH groups of water and glycerol. As a result, ZnO nanoparticles, when incorporated in biocomposite films and interacting with CMC, decrease the free water content and therefore, decrease water accessibility [63]. Numerous studies [60,64] have reported a decrease in moisture content following the inclusion of nanoparticles of ZnO. Similarly, the moisture content of the biocomposite film F3 went down significantly from 22.07 ± 0.19% to 20.43 ± 0.34% during the addition of BCS oil. The repellent effect of non-polar components of BCS oil on water molecules may have hastened the flow of moisture through the films and decreased the moisture content of the film samples [65]. This trend appears to be well established; Hopkins et al. [65] reported similar findings for soy protein-flaxseed oil films. In contrast, an increased TM concentration significantly increased the biocomposite film's moisture content from 29.30 ± 0.22% (F4) to 38.32 ± 0.12% (F6). In agreement with an earlier report by RM and Nair [66], the biodegradable, edible film containing *Hibiscus* mucilage showed a 7.86% increased moisture content. The researchers also concluded that as a hydrocolloid, mucilage retains moisture better, which is helpful for coatings and wrappers to keep fruits fresh for extended periods.

The water activity measurement is essential because it reveals the amount of water that is free from the substrate and consequently available for the growth of microorganisms. According to Table 2, the water activity significantly decreased from 0.21 ± 0.01% (F1) to 0.06 ± 0.01% (F2) during the addition of ZnO nanoparticles in the biocomposite films. A decrease in water activity in the film samples following the addition of ZnO nanoparticles can be attributed to the nanoparticles filling the pores in the CMC film. Rezaei et al. [67] reported that ZnO nanoparticles decreased the water activity in wheat gluten/ZnO nanoparticle films, which confirmed our results. The results also overperformed with an increase in glycerol content. This might be a result of glycerol's capacity to bind water. Glycerol is a polyhydric alcohol humectant that binds to water in food products to change or reduce water activity. In contrast, adding BCS oil to film F3 significantly increased its water activity (0.09 ± 0.02%), possibly due to hydrogen and covalent interactions between the CMC network and the polyphenolic compounds in BCS oil. These processes likely maximize the accessibility of hydrogen groups to form a hydrophilic bond with water, hence increasing the film's affinity. Table 2 shows that water activity increased as the amount of TM increased in the film samples. The soluble fiber of TM presents a high capacity for water retention. Thus, the amount of free water increased with the addition of TM. However, the values found were still lower than in other studies [68,69].

3.1.8. Water Solubility and Water Uptake Capacity

To better understand film behavior when in contact with water, water solubility and water uptake capacity are two critical characteristics of biocomposite films. According to Table 2, the higher water solubility of the biocomposite film F1 (88.96 ± 4.00%) could be explained by the CMC hydrophilic groups and glycerol interacting readily with water. Several reports show higher water solubility for CMC-based films [27,70]. Moreover, with the addition of ZnO nanoparticles, the water solubility value of F2 was significantly reduced to 75.33 ± 2.52%. The solubility reduction exhibited by the ZnO nanoparticles may

have been caused by the aggregation of CMC and ZnO nanoparticles [71]. The same effect of ZnO nanoparticles was also reported on CMC, Chinese yam, ZnO nanoparticles, and glycerol-blended edible films [40], and CMC, okra mucilage, and ZnO nanoparticles-based nanocomposite films [27]. In a similar trend, the water solubility value of F3 (57.45 ± 0.51%) significantly decreased with the addition of BCS oil. These results could be ascribed to a decrease in the films' hydrophilic nature, as well as the interaction between the components of BCS oil and the hydroxyl groups of film, which would reduce the availability of hydroxyl groups for interaction with water molecules, consequently resulting in a more water-resistant film [72]. Similarly, Song et al. [73] found that the water solubility values of active corn/wheat starch film decreased slightly with the addition of lemon oil. When TM at 0.6 g/100 mL level was added to the CMC, ZnO nanoparticles, and BCS oil, the obtained biocomposite film F4 was significantly less soluble than F3 film alone at 45.89 ± 2.77%. However, as the concentration of TM increased beyond the 0.6 g/100 mL level, the solubility decreased significantly.

Interestingly, there was no significant difference between the biocomposite films, 34 ± 2.65% (F5), compared to 37.33 ± 3.21% (F6), at the level of 0.8 g/100 mL and 1.0 g/100 mL. These results concord with Mohammadi et al. [13], who reported a significant decrease in water solubility of CMC, okra mucilage, and ZnO nanoparticles-based nanocomposite films from 65.4 ± 2.8% to 45.81 ± 4.1% with the increasing concentration of okra mucilage. This effect indicated high cohesion matrices by numerous hydrogen bonds between the polysaccharides of TM and BCS oil. Simple sugars present in TM in conjunction with water and glycerol have a plasticizing effect in films. However, the increase of sugar content led to a large fraction of available water bonded by sugars, reducing, in this way, the possibility of interaction with the surrounding water. As a consequence, films incorporating TM presented reduced water solubility. Moreover, water solubility involves an interaction of film components with water through hydrogen bonds, after a swelling of hydrophilic polymers. Additionally, the penetration of water disrupting hydrogen and van der Waals forces between polymer chains affected the film's water solubility [73].

The water uptake capacity of the biocomposite films is given in Table 2. Introducing ZnO nanoparticles and BCS oil to the CMC matrix significantly decreases the biocomposite films' water uptake capacity from 274.67 ± 43.59% (F1) to 152.81 ± 35.41% (F2). The experimental results showed that when the ZnO nanoparticle content of films was increased, more hydrogen bonds formed between the ZnO and the matrix components. For this reason, free water molecules do not interact as strongly with biocomposite films as with composite films alone [74]. On the other hand, the decrease in the value of water uptake with the addition of BCS oil is due to the hydrophobic nature of the essential oil, so the higher the volatile oil content, the lower the absorption of the films to water [75]. These results are consistent with results reported by other researchers on nanocomposites [74,76]. Table 2 shows that films F5 and F6 have absorbed a significantly higher percentage of water (F5: 365 ± 12.87%, F6: 363.92 ± 5.55%), resulting from the binding of hydroxyl groups in the TM with water. The TM's water-soluble fibers can absorb water up to several times its weight [77]. These results showed consistency with the prepared films' moisture content and water activity.

3.1.9. Antioxidant Activity (DPPH Method)

To assess the antioxidant activity of biocomposite films, the DPPH radical scavenging activity method was used and the results are shown in Table 2. The DPPH radical scavenging activities of the prepared films significantly increased to 24.14 ± 0.01%, respectively, when 0.5 g/100 mL ZnO nanoparticles were added. A mechanism to explain the ZnO nanoparticles' antioxidant activity may be the transfer of oxygen electron density to the odd electron on the nitrogen atom in DPPH [78]. The obtained results are the same line as the case of the previous findings by Semi et al. [79]. However, the antioxidant activity of the F3 film increased significantly (31.11 ± 0.04%) when added to 1 g/100 mL of BCS oil. The phenolic compounds have an essential role in enhancing the antioxidant properties of

the BCS oil due to their high potential for inhibiting free radicals [80]. This result confirms Taami et al. [81], who showed similar results in biodegradable starch film formulated with *Bunium persicum* essential oil nanoemulsion. Furthermore, the antioxidant activity of the prepared films dramatically increased from 37.61 ± 0.02% (F4) to 65.63 ± 0.01% (F6), which was statistically significant. The chelating ability and the reducing power of taro increased with mucilage content. Moreover, the antioxidant activity of phenolic compounds in TM is due to their redox characteristics, which allow them to act as singlet oxygen quenchers, hydrogen donors, and reducing agents. They also have metal-chelating potential. Therefore, TM has excellent antioxidant properties [82]. Similar results were obtained by Makhloufi et al. [83] with polysaccharide-based films of cactus mucilage and agar.

3.1.10. Antimicrobial Activity

In the present study, the antimicrobial activity of the prepared films is the inhibition of the growth of foodborne pathogens *Staphylococcus aureus* (a Gram-positive organism) and *Escherichia coli* (a Gram-negative organism), as measured by the diameter of an inhibitory zone (mm). Inhibition zones ensure that the film is more efficient at inhibiting microbial growth by forming a greater inhibition zone. As presented in Figure 5, the film F1 (which consists of CMC and glycerol) did not show any antibacterial activity; however, F2 film with ZnO nanoparticles presented a significant ($p < 0.05$) reduction in cell viability of both *E. coli* and *S. aureus*. Antibacterial activity of the F3 film increased significantly when 1 g/100 mL BCS oil was added. There was a significant inhibitory effect on *E. coli* and *S. aureus* when the films were formulated with different concentrations of TM. Compared to Gram-negative *E. coli*, Gram-positive *S. aureus* caused a more significant decrease in viable cells. Since Gram-negative bacteria have an external lipopolysaccharide wall surrounding their peptidoglycan cell wall, they are more resistant to antimicrobial agents than Gram-positive bacteria [84].

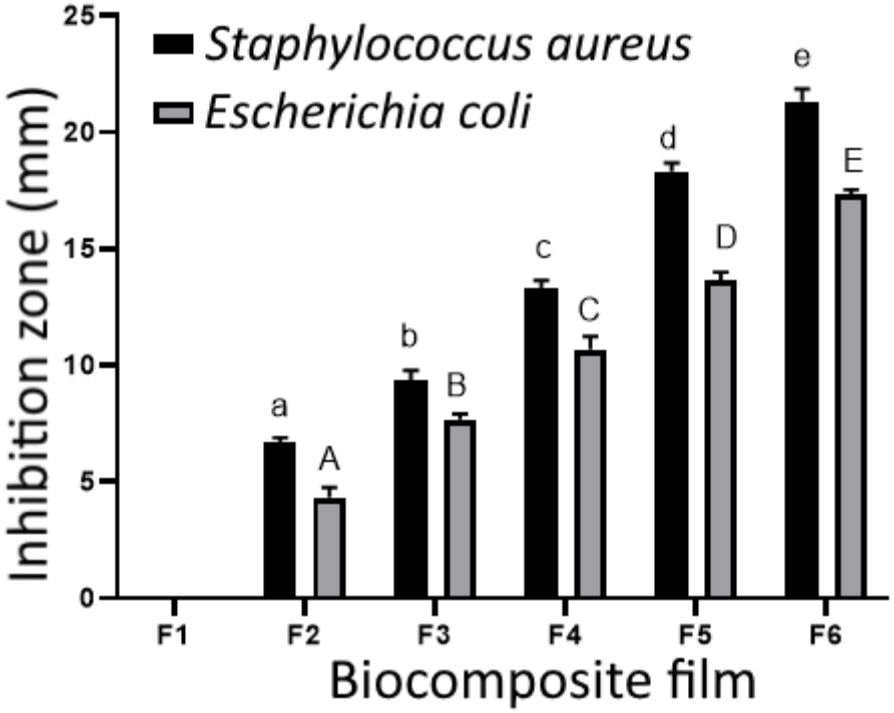

Figure 5. Inhibitory effects of the biocomposite films on *Escherichia coli* and *Staphylococcus aureus.* The same color bars with different letters are statistically different ($p < 0.05$) according to Tukey honestly significant difference test. For sample codes F1 to F6, refer to Table 1.

The effectiveness of ZnO nanoparticles against Gram-positive bacteria is well documented. A further study found that films containing ZnO nanoparticles had more potent

antimicrobial activity against Gram-positive bacteria [85]. According to Anitha et al. [86], ZnO nanoparticles exerted a more significant inhibitory effect on Gram-positive *S. aureus* than the Gram-negative *E. coli*. Other studies have also reported the antimicrobial properties of films containing ZnO nanoparticles [27,55]. There is a possibility that ZnO nanoparticles may directly bind to the outer cell wall of Gram-positive bacteria, which has numerous pores, allowing them to easily penetrate the cell and cause leakage of intracellular contents that may ultimately lead to cell death. Nevertheless, ZnO nanoparticles may not attach readily to the outer cell membrane of Gram-negative bacteria since they contain lipoprotein, lipopolysaccharide, and phospholipids [87]. Furthermore, membrane lipid oxidation of bacteria may also be mediated by reactive oxygen species [40]. On the other hand, the antibacterial effect of BCS oil is primarily attributable to the presence of phenolic compounds, which, by releasing their proton, promote the delocalization of double bonds and ATP in bacteria, as well as the disruption of their cell wall and eventual cell death [88]. Many active compounds have been isolated from BCS oil, including thymoquinone (TQ). TQ (2-isopropyl-5-methyl-1,4-benzoquinone) is the main bioactive compound of BCS oil, showing antibacterial activity [89]. Moreover, researchers have shown that natural antinutrient components, including phytic acid and tannins, affect bacterial growth. Thus, the present study anticipates that significant differences in the antibacterial activity of films containing TM may correlate with the antinutrient contents of the films [27].

4. Conclusions

Biocomposite films containing antioxidant and antimicrobial activity promise to postpone microbial spoilage in food and reduce contamination risks. Additionally, plastic waste disposal has long been the focus of researchers searching for potential biocomposite materials. The combination of plant-based materials could be an adequate substitute for non-biodegradable packaging materials. Hence, given the importance of plant-derived materials-based biocomposite film, the present study intended to prepare CMC/BCS oil/TM-based biocomposite film with antioxidant and antimicrobial activities by incorporating ZnO particles and glycerol using a solution casting method. The key aim was to determine the effect of various concentrations of CMC and TM on the mechanical and physical properties of the biocomposite films. Significant changes in moisture content, water activity, water solubility, water uptake capacity, antioxidative property, tensile strength, elongation at break, surface color, and whiteness index were observed. Noticeable surface morphological differences were observed between the prepared films analyzed by SEM. The FTIR analysis indicated the existence of a -OH group, N-H bond, alkaline group, C-C, C=N, C-H, C-O-H, and C-O-C bond formation, confirming the interaction of CMC, glycerol, BCS oil, ZnO nanoparticles, and TM. Incorporating ZnO nanoparticles, BCS oil, and TM into composite films increased thermal stability and possessed antibacterial effects, inhibiting the growth of Gram-negative (*Escherichia coli*) and Gram-positive (*Staphylococcus aureus*) foodborne pathogens. Based on the results, the present study suggests that the different combinations of CMC, glycerol, ZnO particles, and TM have considerable effects on the properties and performance of the biocomposite films, which can be used as environment-friendly antioxidative and antimicrobial packaging films. Having said that, there are several improvements and research that should be worked on for future endeavors. For instance, it should be necessary to conduct experiments to validate how well the prepared films can protect the texture of real foodstuffs against environmental factors and preserve its color and odor for a long period. Moreover, the optimization of CMC, glycerol, BCS oil, and TM concentrations should be carried out further to increase the efficacy of the prepared biocomposite films. Furthermore, additional studies are required to determine particle sizes, zeta potential, rheological behavior, and acute toxicity of the prepared biocomposite films.

Author Contributions: Conceptualization, T.A., M.R.R. and B.S.I.; methodology, A.B. and T.A.; software, M.M.H., M.F.A., K.S., M.S. and R.A.; validation, M.M.H., M.F.A., K.S., M.S., B.S.I. and M.R.R.; formal analysis, T.A. and A.B.; investigation, T.A. and A.B.; resources, M.R.R. and B.S.I.; data curation, T.A. and A.B.; writing—original draft preparation, T.A. and A.B.; writing—review and editing, B.S.I., K.S., M.R.R. and M.S.; visualization, M.M.H., M.F.A., K.S., M.R.R., B.S.I. and M.S.; supervision, M.R.R. and B.S.I.; project administration, M.R.R. and B.S.I.; funding acquisition, M.R.R., R.A. and B.S.I. All authors have read and agreed to the published version of the manuscript.

Funding: This study received financial support from the promotional research grant (Project ID: AS/2021/1/28) by the Shahjalal University of Science and Technology (SUST) research center.

Institutional Review Board Statement: Not applicable.

Informed Consent Statement: Not applicable.

Data Availability Statement: Data are available within the article.

Acknowledgments: The authors thank Mohammad Abul Hasnat, Department of Chemistry, Shahjalal University of Science and Technology (SUST), for providing synthesized ZnO nanoparticles. The technical support for the film characterization was provided by the Institute of Glass and Ceramic Research and Testing (IGCRT), Bangladesh Council of Scientific and Industrial Research (BCSIR), Institute of Fibre and Polymer Research Division, BCSIR, Department of Biochemistry and Molecular Biology, and the Department of Food Engineering and Tea Technology, SUST, are highly acknowledged.

Conflicts of Interest: The authors declare no conflict of interest.

References

1. Puscaselu, R.; Gutt, G.; Amariei, S. Biopolymer-Based Films Enriched with *Stevia rebaudiana* Used for the Development of Edible and Soluble Packaging. *Coatings* **2019**, *9*, 360. [CrossRef]
2. Martins, V.G.; Palezi, S.C.; Alves-Silva, G.F.; Santos, L.G. Biodegradable Packaging Materials and Techniques to Improve Their Performance. In *Food Packaging: The Smarter Way*; Springer: Singapore, 2022; pp. 61–105.
3. Mesgari, M.; Aalami, A.H.; Sathyapalan, T.; Sahebkar, A. A Comprehensive Review of the Development of Carbohydrate Macromolecules and Copper Oxide Nanocomposite Films in Food Nanopackaging. *Bioinorg. Chem. Appl.* **2022**, *2022*, 7557825. [CrossRef] [PubMed]
4. Liu, Y.; Ahmed, S.; Sameen, D.E.; Wang, Y.; Lu, R.; Dai, J.; Li, S.; Qin, W. A Review of Cellulose and Its Derivatives in Biopolymer-Based for Food Packaging Application. *Trends Food Sci. Technol.* **2021**, *112*, 532–546. [CrossRef]
5. Kostag, M.; El Seoud, O.A. Sustainable Biomaterials Based on Cellulose, Chitin and Chitosan Composites—A Review. *Carbohydr. Polym. Technol. Appl.* **2021**, *2*, 100079. [CrossRef]
6. Nesic, A.; Meseldzija, S.; Cabrera-Barjas, G.; Onjia, A. Novel Biocomposite Films Based on High Methoxyl Pectin Reinforced with Zeolite Y for Food Packaging Applications. *Foods* **2022**, *11*, 360. [CrossRef]
7. Tosif, M.M.; Najda, A.; Klepacka, J.; Bains, A.; Chawla, P.; Kumar, A.; Sharma, M.; Sridhar, K.; Gautam, S.P.; Kaushik, R. A Concise Review on Taro Mucilage: Extraction Techniques, Chemical Composition, Characterization, Applications, and Health Attributes. *Polymers* **2022**, *14*, 1163. [CrossRef]
8. Briones, M.F.; Jazmin, P.F.; Pajarillaga, B.E.; Juvinal, J.G.; DeLeon, A.A.; Rustia, J.M.; Tuates, A.M. Biodegradable Film from Wild Taro *Colocasia Esculenta* (L.) Schott Starch. *Agric. Eng. Int. CIGR J.* **2020**, *22*, 152–155.
9. Roy, S.; Rhim, J.W. Carboxymethyl Cellulose-Based Antioxidant and Antimicrobial Active Packaging Film Incorporated with Curcumin and Zinc Oxide. *Int. J. Biol. Macromol.* **2020**, *148*, 666–676. [CrossRef]
10. Foghara, S.K.; Jafarian, S.; Zomorodi, S.; Asl, A.K.; Nasiraei, L.R. Fabrication and Characterization of an Active Bionanocomposite Film Based on Basil Seed Mucilage and ZnO Nanoparticles. *J. Food Meas. Charact.* **2020**, *14*, 3542–3550. [CrossRef]
11. Sabbah, M.; Altamimi, M.; Di Pierro, P.; Schiraldi, C.; Cammarota, M.; Porta, R. Black Edible Films from Protein-Containing Defatted Cake of *Nigella sativa* Seeds. *Int. J. Mol. Sci.* **2020**, *21*, 832. [CrossRef]
12. Andrade, L.A.; de Oliveira Silva, D.A.; Nunes, C.A.; Pereira, J. Experimental Techniques for the Extraction of Taro Mucilage with Enhanced Emulsifier Properties Using Chemical Characterization. *Food Chem.* **2020**, *327*, 127095. [CrossRef]
13. Wang, L.-F.; Rhim, J.-W.; Hong, S.-I. Preparation of Poly (Lactide)/Poly (Butylene Adipate-Co-Terephthalate) Blend Films Using a Solvent Casting Method and Their Food Packaging Application. *LWT-Food Sci. Technol.* **2016**, *68*, 454–461. [CrossRef]
14. Monjazeb Marvdashti, L.; Koocheki, A.; Yavarmanesh, M. Characterization, Release Profile and Antimicrobial Properties of Bioactive Polyvinyl Alcohol-Alyssum Homolocarpum Seed Gum-Nisin Composite Film. *Food Biophys.* **2019**, *14*, 120–131. [CrossRef]
15. Ghamari, M.A.; Amiri, S.; Rezazadeh-Bari, M.; Rezazad-Bari, L. Physical, Mechanical, and Antimicrobial Properties of Active Edible Film Based on Milk Proteins Incorporated with *Nigella sativa* Essential Oil. *Polym. Bull.* **2022**, *79*, 1097–1117. [CrossRef]
16. Binti Che Wan, N.H.; Nafchi, A.M.; Huda, N. Tensile Strength, Elongation at Breaking Point and Surface Color of a Biodegradable Film Based on a Duck Feet Gelatin and Polyvinyl Alcohol Blend. *Asia Pac. J. Sustain. Agric. Food Energy* **2018**, *6*, 16–21.

17. Rhim, J.-W.; Wang, L.-F. Mechanical and Water Barrier Properties of Agar/κ-Carrageenan/Konjac Glucomannan Ternary Blend Biohydrogel Films. *Carbohydr. Polym.* **2013**, *96*, 71–81. [CrossRef]
18. Fernandes, S.S.; Romani, V.P.; da Silva Filipini, G.; Martins, V.G. Chia Seeds to Develop New Biodegradable Polymers for Food Packaging: Properties and Biodegradability. *Polym. Eng. Sci.* **2020**, *60*, 2214–2223. [CrossRef]
19. Ghazihoseini, S.; Alipoormazandarani, N.; Nafchi, A.M. The Effects of Nano-SiO_2 on Mechanical, Barrier, and Moisture Sorption Isotherm Models of Novel Soluble Soybean Polysaccharide Films. *Int. J. Food Eng.* **2015**, *11*, 833–840. [CrossRef]
20. *ASTM D882-10*; Standard Test Method for Tensile Properties of Thin Plastic Sheeting. American Society for Testing and Materials: West Conshohocken, PA, USA, 2010; Volume 87.
21. Govari, M.; Tryfinopoulou, P.; Panagou, E.Z.; Nychas, G.-J.E. Application of Fourier Transform Infrared (FT-IR) Spectroscopy, Multispectral Imaging (MSI) and Electronic Nose (E-Nose) for the Rapid Evaluation of the Microbiological Quality of Gilthead Sea Bream Fillets. *Foods* **2022**, *11*, 2356. [CrossRef]
22. Ibrahim, S.; Elsayed, H.; Hasanin, M. Biodegradable, Antimicrobial and Antioxidant Biofilm for Active Packaging Based on Extracted Gelatin and Lignocelluloses Biowastes. *J. Polym. Environ.* **2021**, *29*, 472–482. [CrossRef]
23. Kim, H.; Yang, H.-J.; Lee, K.-Y.; Beak, S.-E.; Bin Song, K. Characterization of Red Ginseng Residue Protein Films Incorporated with Hibiscus Extract. *Food Sci. Biotechnol.* **2017**, *26*, 369–374. [CrossRef] [PubMed]
24. Bajpai, S.K.; Chand, N.; Chaurasia, V. Nano Zinc Oxide-Loaded Calcium Alginate Films with Potential Antibacterial Properties. *Food Bioprocess Technol.* **2012**, *5*, 1871–1881. [CrossRef]
25. Ross, J.E.; Scangarella-Oman, N.; Jones, R.N. Determination of Disk Diffusion and MIC Quality Control Guidelines for GSK2251052: A Novel Boron-Containing Antibacterial. *Diagn. Microbiol. Infect. Dis.* **2013**, *75*, 437–439. [CrossRef] [PubMed]
26. Safira, K.R.; Rawdkuen, S. [5-1130-P-07] Properties of Rice Starch-Based Film Incorporated with Zinc Oxide Nanoparticles. In Proceedings of the [5-1130-P] Postharvest/Food Technology and Process Engineering (5th), Sapporo, Japan, 5 September 2019.
27. Mohammadi, H.; Kamkar, A.; Misaghi, A. Nanocomposite Films Based on CMC, Okra Mucilage and ZnO Nanoparticles: Physico Mechanical and Antibacterial Properties. *Carbohydr. Polym.* **2018**, *181*, 351–357. [CrossRef] [PubMed]
28. Oliveira, N.L.; Rodrigues, A.A.; Neves, I.C.O.; Lago, A.M.T.; Borges, S.V.; de Resende, J.V. Development and Characterization of Biodegradable Films Based on Pereskia Aculeata Miller Mucilage. *Ind. Crops Prod.* **2019**, *130*, 499–510. [CrossRef]
29. Fabra, M.J.; Falcó, I.; Randazzo, W.; Sánchez, G.; López-Rubio, A. Antiviral and Antioxidant Properties of Active Alginate Edible Films Containing Phenolic Extracts. *Food Hydrocoll.* **2018**, *81*, 96–103. [CrossRef]
30. Ojagh, S.M.; Rezaei, M.; Razavi, S.H.; Hosseini, S.M.H. Development and Evaluation of a Novel Biodegradable Film Made from Chitosan and Cinnamon Essential Oil with Low Affinity toward Water. *Food Chem.* **2010**, *122*, 161–166. [CrossRef]
31. Atarés, L.; Bonilla, J.; Chiralt, A. Characterization of Sodium Caseinate-Based Edible Films Incorporated with Cinnamon or Ginger Essential Oils. *J. Food Eng.* **2010**, *100*, 678–687. [CrossRef]
32. Wulandari, Y.; Warkoyo, N.H. Characterization of Edible Film from Starch of Taro (*Colocasia Esculenta* (L.) Schott) with Addition of Chitosan on Dodol Substituted Seaweed (*Eucheuma Cottonii* L.). *Food Technol. Halal Sci. J.* **2018**, *1*, 22–32. [CrossRef]
33. Pang, J.; Liu, X.; Zhang, X.; Wu, Y.; Sun, R. Fabrication of Cellulose Film with Enhanced Mechanical Properties in Ionic Liquid 1-Allyl-3-Methylimidaxolium Chloride (AmimCl). *Materials* **2013**, *6*, 1270–1284. [CrossRef]
34. Srikandace, Y.; Andayani, D.G.S.; Karina, M. Preliminary Study of the Degradation of Biocellulose Based Film Using Soil Fungi Aspergillus Unguis TP3 and Paecilomyces Marquandii TP4 Producing Cellulose. *IOP Conf. Ser. Earth Environ. Sci.* **2019**, *277*, 12001. [CrossRef]
35. Kanmani, P.; Rhim, J.-W. Properties and Characterization of Bionanocomposite Films Prepared with Various Biopolymers and ZnO Nanoparticles. *Carbohydr. Polym.* **2014**, *106*, 190–199. [CrossRef]
36. Shankar, S.; Teng, X.; Rhim, J.-W. Effects of Concentration of ZnO Nanoparticles on Mechanical, Optical, Thermal, and Antimicrobial Properties of Gelatin/ZnO Nanocomposite Films. *Korean J. Packag. Sci. Technol.* **2014**, *20*, 41–49.
37. Muñoz-Tébar, N.; Carmona, M.; de Elguea-Culebras, G.; Molina, A.; Berruga, M.I. Chia Seed Mucilage Edible Films with Origanum Vulgare and Satureja Montana Essential Oils: Characterization and Antifungal Properties. *Membranes* **2022**, *12*, 213. [CrossRef]
38. Wang, R.; Li, X.; Liu, L.; Chen, W.; Bai, J.; Ma, F.; Liu, X.; Kang, W. Preparation and Characterization of Edible Films Composed of Dioscorea Opposita Thunb. Mucilage and Starch. *Polym. Test.* **2020**, *90*, 106708. [CrossRef]
39. Tosif, M.M.; Najda, A.; Bains, A.; Zawiślak, G.; Maj, G.; Chawla, P. Starch–Mucilage Composite Films: An Inclusive on Physicochemical and Biological Perspective. *Polymers* **2021**, *13*, 2588. [CrossRef]
40. Li, X.; Ren, Z.; Wang, R.; Liu, L.; Zhang, J.; Ma, F.; Khan, M.Z.H.; Zhao, D.; Liu, X. Characterization and Antibacterial Activity of Edible Films Based on Carboxymethyl Cellulose, Dioscorea Opposita Mucilage, Glycerol and ZnO Nanoparticles. *Food Chem.* **2021**, *349*, 129208. [CrossRef]
41. Yan, Q.-L.; Cohen, A.; Petrutik, N.; Shlomovich, A.; Burstein, L.; Pang, S.-P.; Gozin, M. Highly Insensitive and Thermostable Energetic Coordination Nanomaterials Based on Functionalized Graphene Oxides. *J. Mater. Chem. A* **2016**, *4*, 9941–9948. [CrossRef]
42. Esteghlal, S.; Niakousari, M.; Hosseini, S.M.H. Physical and Mechanical Properties of Gelatin-CMC Composite Films under the Influence of Electrostatic Interactions. *Int. J. Biol. Macromol.* **2018**, *114*, 1–9. [CrossRef]
43. Araújo, A.; Galvão, A.; Silva Filho, C.; Mendes, F.; Oliveira, M.; Barbosa, F.; Sousa Filho, M.; Bastos, M. Okra Mucilage and Corn Starch Bio-Based Film to Be Applied in Food. *Polym. Test.* **2018**, *71*, 352–361. [CrossRef]
44. Mujtaba, M.; Akyuz, L.; Koc, B.; Kaya, M.; Ilk, S.; Cansaran-Duman, D.; Martinez, A.S.; Cakmak, Y.S.; Labidi, J.; Boufi, S. Novel, Multifunctional Mucilage Composite Films Incorporated with Cellulose Nanofibers. *Food Hydrocoll.* **2019**, *89*, 20–28. [CrossRef]

45. Dick, M.; Costa, T.M.H.; Gomaa, A.; Subirade, M.; de Oliveira Rios, A.; Flôres, S.H. Edible Film Production from Chia Seed Mucilage: Effect of Glycerol Concentration on Its Physicochemical and Mechanical Properties. *Carbohydr. Polym.* **2015**, *130*, 198–205. [CrossRef] [PubMed]
46. Tantiwatcharothai, S.; Prachayawarakorn, J. Property Improvement of Antibacterial Wound Dressing from Basil Seed (O. *Basilicum* L.) Mucilage-ZnO Nanocomposite by Borax Crosslinking. *Carbohydr. Polym.* **2020**, *227*, 115360. [CrossRef] [PubMed]
47. Kurd, F.; Fathi, M.; Shekarchizadeh, H. Basil Seed Mucilage as a New Source for Electrospinning: Production and Physicochemical Characterization. *Int. J. Biol. Macromol.* **2017**, *95*, 689–695. [CrossRef] [PubMed]
48. Damas, M.S.P.; Pereira Junior, V.A.; Nishihora, R.K.; Quadri, M.G.N. Edible Films from Mucilage of C Ereus Hildmannianus Fruits: Development and Characterization. *J. Appl. Polym. Sci.* **2017**, *134*, 45223. [CrossRef]
49. López-Garciia, F.; Arzate-Vázquez, I.; Guzmán-Lucero, D.; Terrés-Rojas, E.; Cabrero-Palomino, D.; Maciel-Cerda, A.; Jiménez-Martínez, C.; Delgado-Macuil, R. Physical and Chemical Characterization of a Biopolymer Film Made with Corn Starch and Nopal Xoconostle (Opuntia Joconsotle) Mucilage. *Rev. Mex. Ing. Química* **2017**, *16*, 147–158. [CrossRef]
50. Tongnuanchan, P.; Benjakul, S.; Prodpran, T. Structural, Morphological and Thermal Behaviour Characterisations of Fish Gelatin Film Incorporated with Basil and Citronella Essential Oils as Affected by Surfactants. *Food Hydrocoll.* **2014**, *41*, 33–43. [CrossRef]
51. El-Sayed, S.; Mahmoud, K.H.; Fatah, A.A.; Hassen, A. DSC, TGA and Dielectric Properties of Carboxymethyl Cellulose/Polyvinyl Alcohol Blends. *Phys. B Condens. Matter* **2011**, *406*, 4068–4076. [CrossRef]
52. Archana, G.; Sabina, K.; Babuskin, S.; Radhakrishnan, K.; Fayidh, M.A.; Babu, P.A.S.; Sivarajan, M.; Sukumar, M. Preparation and Characterization of Mucilage Polysaccharide for Biomedical Applications. *Carbohydr. Polym.* **2013**, *98*, 89–94. [CrossRef]
53. Perdones, Á.; Vargas, M.; Atarés, L.; Chiralt, A. Physical, Antioxidant and Antimicrobial Properties of Chitosan–Cinnamon Leaf Oil Films as Affected by Oleic Acid. *Food Hydrocoll.* **2014**, *36*, 256–264. [CrossRef]
54. Tongnuanchan, P.; Benjakul, S.; Prodpran, T. Physico-Chemical Properties, Morphology and Antioxidant Activity of Film from Fish Skin Gelatin Incorporated with Root Essential Oils. *J. Food Eng.* **2013**, *117*, 350–360. [CrossRef]
55. Praseptiangga, D.; Mufida, N.; Panatarani, C.; Joni, I.M. Enhanced Multi Functionality of Semi-Refined Iota Carrageenan as Food Packaging Material by Incorporating SiO_2 and ZnO Nanoparticles. *Heliyon* **2021**, *7*, e06963. [CrossRef]
56. Lee, J.Y.; Garcia, C.V.; Shin, G.H.; Kim, J.T. Antibacterial and Antioxidant Properties of Hydroxypropyl Methylcellulose-Based Active Composite Films Incorporating Oregano Essential Oil Nanoemulsions. *LWT* **2019**, *106*, 164–171. [CrossRef]
57. Aji, A.I.; Praseptiangga, D.; Rochima, E.; Joni, I.M.; Panatarani, C. Optical Transparency and Mechanical Properties of Semi-Refined Iota Carrageenan Film Reinforced with SiO_2 as Food Packaging Material. *AIP Conf. Proc.* **2018**, *1927*, 030039.
58. Venkatesan, R.; Rajeswari, N.; Thendral Thiyagu, T. Preparation, Characterization and Mechanical Properties of k-Carrageenan/SiO_2 Nanocomposite Films for Antimicrobial Food Packaging. *Bull. Mater. Sci.* **2017**, *40*, 609–614. [CrossRef]
59. Sani, I.K.; Pirsa, S.; Tağı, Ş. Preparation of Chitosan/Zinc Oxide/Melissa Officinalis Essential Oil Nano-Composite Film and Evaluation of Physical, Mechanical and Antimicrobial Properties by Response Surface Method. *Polym. Test.* **2019**, *79*, 106004. [CrossRef]
60. Ngo, T.M.P.; Dang, T.M.Q.; Tran, T.X.; Rachtanapun, P. Effects of Zinc Oxide Nanoparticles on the Properties of Pectin/Alginate Edible Films. *Int. J. Polym. Sci.* **2018**, *2018*, 5645797. [CrossRef]
61. Sharma, S.; Barkauskaite, S.; Jaiswal, S.; Duffy, B.; Jaiswal, A.K. Development of Essential Oil Incorporated Active Film Based on Biodegradable Blends of Poly (Lactide)/Poly (Butylene Adipate-Co-Terephthalate) for Food Packaging Application. *J. Packag. Technol. Res.* **2020**, *4*, 235–245. [CrossRef]
62. Luo, M.; Cao, Y.; Wang, W.; Chen, X.; Cai, J.; Wang, L.; Xiao, J. Sustained-Release Antimicrobial Gelatin Film: Effect of Chia Mucilage on Physicochemical and Antimicrobial Properties. *Food Hydrocoll.* **2019**, *87*, 783–791. [CrossRef]
63. Müller, C.M.O.; Laurindo, J.B.; Yamashita, F. Effect of Nanoclay Incorporation Method on Mechanical and Water Vapor Barrier Properties of Starch-Based Films. *Ind. Crops Prod.* **2011**, *33*, 605–610. [CrossRef]
64. Vaezi, K.; Asadpour, G.; Sharifi, H. Effect of ZnO Nanoparticles on the Mechanical, Barrier and Optical Properties of Thermoplastic Cationic Starch/Montmorillonite Biodegradable Films. *Int. J. Biol. Macromol.* **2019**, *124*, 519–529. [CrossRef]
65. Pirnia, M.; Shirani, K.; Yazdi, F.T.; Moratazavi, S.A.; Mohebbi, M. Characterization of Antioxidant Active Biopolymer Bilayer Film Based on Gelatin-Frankincense Incorporated with Ascorbic Acid and Hyssopus Officinalis Essential Oil. *Food Chem. X* **2022**, *14*, 100300. [CrossRef] [PubMed]
66. RM, V.; Nair, B.R. Development and characterisation of edible films based on the mucilage of hibiscus rosa-sinensis linn. (malvaceae). *Int. J. Creat. Res. Thoughts* **2018**, *6*, 542–556.
67. Rezaei, M.; Pirsa, S.; Chavoshizadeh, S. Photocatalytic/Antimicrobial Active Film Based on Wheat Gluten/ZnO Nanoparticles. *J. Inorg. Organomet. Polym. Mater.* **2020**, *30*, 2654–2665. [CrossRef]
68. Amin, M.H.H.; Elbeltagy, A.E.; Mustafa, M.; Khalil, A.H. Development of Low Fat Mayonnaise Containing Different Types and Levels of Hydrocolloid Gum. *J. Agroaliment. Process. Technol.* **2014**, *20*, 54–63.
69. Tee, Y.B.; Tee, L.T.; Daengprok, W.; Talib, R.A. Chemical, Physical, and Barrier Properties of Edible Film from Flaxseed Mucilage. *BioResources* **2017**, *12*, 6656–6664. [CrossRef]
70. Tong, Q.; Xiao, Q.; Lim, L.-T. Preparation and Properties of Pullulan–Alginate–Carboxymethylcellulose Blend Films. *Food Res. Int.* **2008**, *41*, 1007–1014. [CrossRef]
71. Ma, F.; Wang, R.; Li, X.; Kang, W.; Bell, A.E.; Zhao, D.; Liu, X.; Chen, W. Physical Properties of Mucilage Polysaccharides from Dioscorea Opposita Thunb. *Food Chem.* **2020**, *311*, 126039. [CrossRef]

72. Hafsa, J.; Smach, M.A.; Ben Khedher, M.R.; Charfeddine, B.; Limem, K.; Majdoub, H.; Rouatbi, S. Physical, Antioxidant and Antimicrobial Properties of Chitosan Films Containing Eucalyptus Globulus Essential Oil. *LWT-Food Sci. Technol.* **2016**, *68*, 356–364. [CrossRef]
73. Guadarrama-Lezama, A.Y.; Castaño, J.; Velázquez, G.; Carrillo-Navas, H.; Alvarez–Ramírez, J. Effect of Nopal Mucilage Addition on Physical, Barrier and Mechanical Properties of Citric Pectin-Based Films. *J. Food Sci. Technol.* **2018**, *55*, 3739–3748. [CrossRef]
74. Nafchi, A.M.; Nassiri, R.; Sheibani, S.; Ariffin, F.; Karim, A.A. Preparation and Characterization of Bionanocomposite Films Filled with Nanorod-Rich Zinc Oxide. *Carbohydr. Polym.* **2013**, *96*, 233–239. [CrossRef]
75. Sihombing, N.; Elma, M.; Thala'ah, R.N.; Simatupang, F.A.; Pradana, E.A.; Rahma, A. Garlic Essential Oil as an Edible Film Antibacterial Agent Derived from Nagara Sweet Potato Starch Applied for Packaging of Indonesian Traditional Food-Dodol. *IOP Conf. Ser. Earth Environ. Sci.* **2022**, *999*, 12026. [CrossRef]
76. Syafiq, R.; Sapuan, S.M.; Zuhri, M.R.M. Antimicrobial Activity, Physical, Mechanical and Barrier Properties of Sugar Palm Based Nanocellulose/Starch Biocomposite Films Incorporated with Cinnamon Essential Oil. *J. Mater. Res. Technol.* **2021**, *11*, 144–157. [CrossRef]
77. Figuerola, F.; Hurtado, M.L.; Estévez, A.M.; Chiffelle, I.; Asenjo, F. Fibre Concentrates from Apple Pomace and Citrus Peel as Potential Fibre Sources for Food Enrichment. *Food Chem.* **2005**, *91*, 395–401. [CrossRef]
78. Abdolsattari, P.; Rezazadeh-Bari, M.; Pirsa, S. Smart Film Based on Polylactic Acid, Modified with Polyaniline/ZnO/CuO: Investigation of Physicochemical Properties and Its Use of Intelligent Packaging of Orange Juice. *Food Bioprocess Technol.* **2022**, *15*, 2803–2825. [CrossRef]
79. Saemi, R.; Taghavi, E.; Jafarizadeh-Malmiri, H.; Anarjan, N. Fabrication of Green ZnO Nanoparticles Using Walnut Leaf Extract to Develop an Antibacterial Film Based on Polyethylene–Starch–ZnO NPs. *Green Process. Synth.* **2021**, *10*, 112–124. [CrossRef]
80. Bordoni, L.; Fedeli, D.; Nasuti, C.; Maggi, F.; Papa, F.; Wabitsch, M.; DeCaterina, R.; Gabbianelli, R. Antioxidant and Anti-Inflammatory Properties of Nigella Sativa Oil in Human Pre-Adipocytes. *Antioxidants* **2019**, *8*, 51. [CrossRef]
81. Taami, B.; Rostami Zadeh, K.; Aminzare, M.; Hassanzad Azar, H. Antioxidant Efficacy of Biodegradable Starch Film Containing of *Bunium persicum* Essential Oil Nanoemulsion Fortified with Cinnamaldehyde. *J. Med. Plants By-Prod.* **2021**, *2*, 2–9. [CrossRef]
82. Mohite, A.M.; Chandel, D. Formulation of Edible Films from Fenugreek Mucilage and Taro Starch. *SN Appl. Sci.* **2020**, *2*, 1900. [CrossRef]
83. Makhloufi, N.; Chougui, N.; Rezgui, F.; Benramdane, E.; Silvestre, A.J.D.; Freire, C.S.R.; Vilela, C. Polysaccharide-Based Films of Cactus Mucilage and Agar with Antioxidant Properties for Active Food Packaging. *Polym. Bull.* **2022**, *79*, 11369–11388. [CrossRef]
84. Capitani, M.I.; Matus-Basto, A.; Ruiz-Ruiz, J.C.; Santiago-García, J.L.; Betancur-Ancona, D.A.; Nolasco, S.M.; Tomás, M.C.; Segura-Campos, M.R. Characterization of Biodegradable Films Based on *Salvia Hispanica* L. Protein and Mucilage. *Food Bioprocess Technol.* **2016**, *9*, 1276–1286. [CrossRef]
85. Lefatshe, K.; Muiva, C.M.; Kebaabetswe, L.P. Extraction of Nanocellulose and In-Situ Casting of ZnO/Cellulose Nanocomposite with Enhanced Photocatalytic and Antibacterial Activity. *Carbohydr. Polym.* **2017**, *164*, 301–308. [CrossRef] [PubMed]
86. Anitha, S.; Brabu, B.; Thiruvadigal, D.J.; Gopalakrishnan, C.; Natarajan, T.S. Optical, Bactericidal and Water Repellent Properties of Electrospun Nano-Composite Membranes of Cellulose Acetate and ZnO. *Carbohydr. Polym.* **2012**, *87*, 1065–1072. [CrossRef]
87. Li, X.; Feng, X.; Yang, S.; Fu, G.; Wang, T.; Su, Z. Chitosan Kills *Escherichia coli* through Damage to Be of Cell Membrane Mechanism. *Carbohydr. Polym.* **2010**, *79*, 493–499. [CrossRef]
88. Gyawali, R.; Ibrahim, S.A. Natural Products as Antimicrobial Agents. *Food Control* **2014**, *46*, 412–429. [CrossRef]
89. Emeka, L.B.; Emeka, P.M.; Khan, T.M. Antimicrobial Activity of *Nigella sativa* L. Seed Oil against Multi-Drug Resistant Staphylococcus Aureus Isolated from Diabetic Wounds. *Pak. J. Pharm. Sci.* **2015**, *28*, 1985–1990.